HHS Public Access

Author manuscript

Nat Neurosci. Author manuscript; available in PMC 2010 June 01.

Published in final edited form as:

Nat Neurosci. 2009 December ; 12(12): 1524–1533. doi:10.1038/nn.2416.

Adult generation of glutamatergic olfactory bulb interneurons

Monika S. Brill[1,2,10,11], **Jovica Ninkovic**[2,10,11], **Eleanor Winpenny**[3,11], **Rebecca D. Hodge**[5,11], **Ilknur Ozen**[3], **Roderick Yang**[5], **Alexandra Lepier**[1], **Sergio Gascón**[1,2], **Ferenc Erdelyi**[6], **Gabor Szabo**[6], **Carlos Parras**[7,8], **Francois Guillemot**[7], **Michael Frotscher**[9], **Benedikt Berninger**[1,2], **Robert F. Hevner**[5], **Olivier Raineteau**[3,4], and **Magdalena Götz**[1,2,10]

[1] Department of Physiological Genomics, Institute of Physiology, Ludwig-Maximilians University Munich, Schillerstrasse 46, D-80336 Munich, Germany

[2] Institute for Stem Cell Research, Helmholtz Zentrum München, German Research Center for Environmental Health, Ingolstädter Landstrasse 1, D-85764 Neuherberg, Germany

[3] Cambridge Centre for Brain Repair, Robinson Way, Cambridge, CB2 2PY, UK

[5] Departments of Neurological Surgery and Pathology, University of Washington, Seattle Children's Hospital Research Institute, 1900 Ninth Ave, Seattle WA 98101, USA

[6] Laboratory of Molecular Biology and Genetics, Institute of Experimental Medicine, P.O. Box 67, H-1450 Budapest, Hungary

[7] Division of Molecular Neurobiology, MRC- National Institute for Medical Research, The Ridgeway, Mill Hill, London, NW7 1AA, UK

[9] Insitute of Anatomy and Cell Biology University of Freiburg, D-79001 Freiburg, Germany

[10] Munich Center for Integrated Protein Science CiPS[M]

Abstract

The adult mouse subependymal zone (SEZ) harbours neural stem cells that are thought to generate exclusively GABAergic interneurons of the olfactory bulb. Here we describe the adult generation of glutamatergic juxtaglomerular neurons, with dendritic arborizations that project into adjacent glomeruli identifying them as short-axon cells. Fate mapping revealed that these originate from

Correspondence should be addressed to M. G. (magdalena.goetz@helmholtz-muenchen.de), O. R. (raineteau@hifo.uzh.ch) or R. F. H. (rhevner@u.washington.edu).

[4]Present address: Brain Research Institute, Universtiy of Zürich/ETH, Winterthurstrasse 190, 8057 Zürich, Switzerland

[8]Present address: INSERM U711, Biologie des Interactions Neurones/Glie, Hôpital de la Pitié-Salpêtrière, 47, Boulevard de l'Hôpital, Batiment de la Pharmacie, 75651 Paris, France

[11]These authors contributed equally to this work

Author contributions

M.S.B., O.R. and R. D. H. made the original observation of glutamatergic progenitors in the SEZ; M.S.B. conducted most experiments; J.N., E.W., O. R. and R.D.H. conducted experiments crucial for the identification of adult generated glutamatergic neurons in the olfactory bulb; I.O. and R.Y. contributed to experiments using *Neurog2*$^{GFP/+}$ and *Tbr2*$^{BAC\text{-}GFP}$ mice respectively; A.L. and S.G. designed and produced the viral vectors; F.E. and G.S. provided the *GAD65-GFP* mice; C.P. contributed with experiments using *Ngn2*$^{+/GFP}$ and *Mash1*$^{BAC\text{-}GFP}$; F.G. provided the *Neurog2*$^{GFP/+}$ and *E1-Neurog2-Cre* mice; M.F. designed the electron microscopy experiments and analyzed the data; B.B. designed and conducted all electrophysiological experiments; R.F.H., O.R. and M.G. supervised the project and designed experiments. M.G. wrote the manuscript; M.S. B., B.B., R.D.H., R.F.H. and O.R. contributed to the writing of the manuscript.

Neurogenin2- and Tbr2-expressing progenitors located in the dorsal region of the SEZ. Progenitors of these glutamatergic interneurons recapitulate the sequential expression of transcription factors that hallmark glutamatergic neurogenesis in the developing cerebral cortex and adult hippocampus. Indeed, the molecular specification of these SEZ progenitors allows for their recruitment into the cerebral cortex upon lesion. Taken together, our data show that SEZ progenitors not only produce a novel population of adult-born glutamatergic juxtaglomerular neurons, but may also provide a new source of progenitors for endogenous repair.

The presence of neural stem cells (NSCs) in the adult mammalian brain has prompted hope for replacement of degenerating neurons. This potential avenue for repair has been further supported by the observation that neuroblasts originating from these NSCs are recruited to sites of injury1, 2. Adult neurogenesis occurs largely in two regions of the forebrain that generate distinct types of neurons: the subgranular zone generating glutamatergic projection neurons of the dentate gyrus and the subependymal zone (SEZ) generating GABAergic interneurons of the olfactory bulb3. The potential of these regions to contribute to endogenous repair may depend on the range of neuronal subtypes they can produce. While earlier transplantation studies had proposed a broad potential of NSCs in regard to the generation of different neuronal subtypes4, this view has recently been challenged by the demonstration of distinct NSCs with restricted potential regarding subtype specification5. On the other hand, it has been suggested that apoptotic cell death in the cerebral cortex elicits the migration of neuroblasts from the SEZ with the ability to replace glutamatergic projection neurons6, 7. Given that SEZ cells have so far been thought to generate only GABAergic neurons this recruitment either suggests a high degree of plasticity of adult SEZ cells or, alternatively, there might be a yet undefined source of glutamatergic neurons in this region.

NSCs in the adult SEZ generate GABAergic interneurons integrating into the granule cell layer (GCL) or glomerular layer of the olfactory bulb8. A large part of these interneurons arise from the lateral SEZ that derives from the ventral telencephalon producing most telencephalic GABAergic neurons during development8, 9. Transcription factors crucial for the generation of GABAergic interneurons during development, such as Dlx10 and Sp811, continue to determine the postnatal and adult generation of olfactory bulb interneurons10, 11. Transcription factors present in the dorsal telencephalon during development, such as Pax6 or (Neurogenin2) Neurog212, are largely restricted in their expression to the dorsal region of the adult10, 13 or postnatal SEZ14. Fate-mapping experiments showed that the adult dorsal SEZ originates from the Emx1-positive area of the embryonic telencephalon and participates in the generation of specific subtypes of GABAergic olfactory neurons, such as the dopaminergic periglomerular neurons15, 16.

However, during embryonic development, dorsal progenitors generate predominantly glutamatergic neurons, in a Pax6-dependent manner, including those of the olfactory bulb17, 18. Thus, the entire population of olfactory bulb projection neurons is thought to derive from a Pax6-expressing territory19. In the developing cerebral cortex, Pax6 regulates Neurogenin1 (Neurog1) and Neurogenin2 (Neurog2) expression and these transcription factors are important to specify cortical neurons towards a glutamatergic fate17, 18, 20. In

addition, the transcription factors Tbr1 and Tbr2 (also known as Eomes) are expressed in early post-mitotic glutamatergic neurons and their intermediate progenitors21. Given the glutamatergic progeny of the dorsal telencephalon during development and its contribution to the adult SEZ, we searched and found progenitors generating glutamatergic neurons in the adult dorsal SEZ.

Results

Neurog2 and Tbr2 in a subset of dorsal SEZ progenitors

Consistent with the above hypothesis, we detected Neurog2- and Tbr2-immunoreactive cells in a dorsal subregion of the SEZ and the rostral migratory stream (RMS) (Fig. 1a–d; Supplementary Fig. 1), while Pax6- and Mash1 (also known as Ascl1)-expressing progenitors were distributed in a more wide-spread manner (Supplementary Fig. 2a). Consistent with their similar localization, most Neurog2-expressing cells (using Supplementary Fig. 1a–d; GFP expressing cells in mice where GFP had been knocked in the *Neurog2* locus referred to thereafter as *Neurog2*$^{+/GFP}$) were either Tbr2- or Tbr1-immunopositive (Tbr2: 96%, 394 *Neurog2*$^{+/GFP}$ cells; Tbr1: 70%, 151 *Neurog2*$^{+/GFP}$ cells; Fig. 1e,f). To further examine their identity, we double-stained for doublecortin (Dcx), a protein exclusively present in neuroblasts and young post-mitotic neurons. The majority of *Neurog2*$^{+/GFP}$+ (80 ± 4%, 212 *Neurog2*$^{+/GFP}$ cells), Tbr2+ (70 ± 8%, 255 cells) and Tbr1+ (Tbr1+, 97 ± 2%, 265 cells) cells were also Dcx+ (Fig. 2a–c). To distinguish post-mitotic neuroblasts from proliferating neuronal progenitors we stained for Ki67, a protein present in dividing cells, or provided the DNA-base analogue BrdU that is incorporated in proliferating cells. Tbr1+ cells were negative for Ki67-immunoreactivity and had not incorporated BrdU a few hours after injection (Fig. 2f,g; 1 ± 1%, 201 cells), suggesting that virtually all Tbr1+ cells are post-mitotic neurons. Conversely, 37% of *Neurog2*$^{+/GFP}$+ cells (156 cells) colocalized with Ki67 and 22% were labelled with BrdU (Fig. 2d,g), indicating that one third of these cells comprise an actively dividing progenitor population. Likewise, a small subset of Tbr2+ cells incorporated BrdU (Fig. 2e,g). During development, Tbr2 is contained mostly in progenitors undergoing a last round of cell division while Tbr1 is in post-mitotic neurons21, 22. To examined whether Tbr1+ cells arise from proliferating progenitors we gave BrdU and waited for 3 days. This protocol resulted in a quarter of all Tbr1+ cells labelled with BrdU (Fig. 2g), consistent with Tbr1 being expressed when cells become post-mitotic. To ensure that Tbr1+ neuroblasts originate from Tbr2+ progenitors, we used the *Tbr2*$^{BAC\text{-}GFP}$ mice23 (Supplementary Fig. 3a–d) allowing short-term fate mapping due to the longer persistence of GFP than Tbr224. Indeed, almost all Tbr1-immunoreactive cells in the RMS were GFP+ (Supplementary Fig. 3e,f), consistent with their origin from Tbr2-expressing progenitors.

Notably, none of these transcription factors (Neurog2, Tbr2, Tbr1) were ever colocalized with Gfap, a protein characteristic for astroglia including NSCs (data not shown). However, Tbr-expressing cells are derived from astrocyte-like NSCs as demonstrated by genetic fate mapping with *GLAST::CreERT2* mediating recombination in *GLAST*+ NSCs25 (Supplementary Fig. 4a). Consistent with the recombination frequency observed upon Tamoxifen-induced recombination25, 26, more than 60% of Tbr2+ cells are GFP+, i.e.

derived from astrocyte-like NSCs. (Tbr2/reporter+ of Tbr2+ 64%, 104 cells). Thus, an adult NSC-derived subpopulation of actively dividing progenitors and young neuroblasts within the SEZ and RMS express a series of transcription factors that are normally indicative of a glutamatergic neuronal lineage.

To examine whether Tbr1+ or Tbr2+ neuroblasts may nevertheless exhibit GABAergic traits we analyzed Dcx+ neuroblasts in the RMS. While most neuroblasts already express GAD and synthesize GABA27 and are GFP+ in *GAD67::GFP*28 and *GAD65-GFP*29 mice in which GFP protein expression is confined to cells expressing *GAD67* or *65* mRNA (Fig. 3a–c), Tbr1/2+ cells define a neuroblast subset negative for both *GAD67*- (Fig. 3d–g) and *GAD65*-driven GFP (Fig. 3h). Consistently, Tbr+ cells did not contain Dlx (Fig. 3i). Moreover, also in the olfactory bulb, Tbr2+ cells did not colocalize with any GABAergic interneuron marker, such as tyrosine hydroxylase, calbindin or calretinin (Supplementary Fig. 5). Thus, neither Tbr1/2+ neuroblasts in the RMS nor the neurons in the olfactory bulb express any traits of GABAergic neurons, suggesting that the Tbr-expressing neuroblasts may be predisposed to differentiate along a different, possibly glutamatergic, phenotype.

Progeny of Tbr2-expressing neuroblasts arrive in the olfactory bulb

While Tbr2 and Tbr1 are clearly contained in migrating neuroblasts within the RMS, hardly any of the Tbr2- or Tbr1-immunoreactive cells present in the glomerular layer of the olfactory bulb were BrdU labelled at postnatal or adult stages (Supplementary Fig. 6a,b), while they could be readily labelled by injection of BrdU at embryonic stages (Supplementary Fig. 6c). Thus, Tbr+ cells in the olfactory bulb are generated during embryonic development. This implies that the Tbr2+ dividing progenitors present in the adult RMS either do not arrive or survive in the adult olfactory bulb, or, alternatively, that the expression of these transcription factors is transient and lost upon arrival.

To distinguish between these possibilities and to elucidate the fate of the Tbr2+ progenitors in the RMS, we followed their progeny using the above described *Tbr2*$^{BAC\text{-}GFP}$ mouse line for short-term fate mapping. GFP/Dcx double-positive cells were present within the RMS at the entrance to the olfactory bulb (Fig. 4a,b) and distributed towards the glomerular layer (Fig. 4c). Some GFP+ cells in the glomerular layer had incorporated BrdU following 3 weeks administration in the drinking water (Fig. 4d–i), suggesting that the progeny of the adult dividing Tbr2+ progenitors arrives indeed in the olfactory bulb, where these cells then down-regulate Tbr2 (Fig. 4j–m) and Tbr1 protein (data not shown). Consistently, *Tbr2*-driven GFP vanishes with a delay, as reflected by the lower GFP-levels in a few juxtaglomerular cells generated and labelled by BrdU 3 weeks earlier and meanwhile negative for Tbr2 protein (Fig. 4j–m).

Adult Neurog2+ progenitors generate glutamatergic neurons

In order to follow the neuronal differentiation of Neurog2/Tbr2-expressing progenitors into later stages by a permanent marker, we utilized Cre-mediated recombination to turn on a persistent reporter gene. As virtually all Neurog2-positive progenitors expressed Tbr1/2 (Fig. 1e,f), we used a mouse line expressing Cre under control of the *Neurog2* enhancer-element 130 (*E1- Neurog2/Cre*) crossed with the *Z/EG*25 reporter line (referred to as *E1-*

Neurog2/CreZ/EG). As expected, *Neurog2-Cre* induced GFP was detected in cells stained for Tbr1 in the RMS (Supplementary Fig. 7a–c) and reporter-positive cells were not detectable in the ventral and lateral SEZ, while present in the dentate gyrus (Supplementary Fig. 7d).

To assess whether adult generated cells of the Neurog2-lineage can be found within the olfactory bulb, we stained for Dcx labelling newly generated neurons. GFP/Dcx double-positive cells were indeed found in the glomerular layer of the olfactory bulb (Fig. 4n). To confirm that these cells are adult generated, we analyzed GFP+ cells for incorporation of BrdU (3 weeks in drinking water followed by a 3 weeks BrdU-free period). Many BrdU/GFP double-positive cells were encountered in the glomerular layer (Fig. 4o–z) amounting to 5% of the entire population of BrdU-positive (BrdU+) cells there (Supplementary Fig. 8e). Thus, a small population of adult generated juxtaglomerular neurons is derived from a Neurog2-expressing lineage.

Adult generation of glutamatergic short-axon cells

In some cases, GFP-expression in *E1-Neurog2/CreZ/EG* allowed for the assessment of the dendritic morphology of the GFP+ neurons labelled by adult BrdU-incorporation. 3D-reconstruction of these BrdU/GFP double-labelled cells from serial sections revealed dendritic arbors extending over 2–3 neighbouring glomeruli (Fig. 4r–t), a morphology typical for short-axon cells, a type of juxtaglomerular neuron mediating glutamatergic transmission between glomeruli31.

To further corroborate the adult generation of these juxtaglomerular neurons we used viral vector-mediated lineage tracing. GFP-containing viral vectors were injected into the ventricle of 3–4 weeks old (lentiviral vectors, Fig. 5a–l) or into the dorsal SEZ of adult mice (MLV-based retroviral vectors, Fig. 5m–q), and GFP-labelled progeny was examined 6 weeks later in the glomerular layer (Fig. 5a,h,m). Very similar to cells labelled by *Neurog2-Cre* fate mapping, some of these virally transduced neurons settling in the vicinity of the glomeruli exhibited long dendritic projections between different glomeruli. In order to examine whether the GFP+ cells with this short-axon-cell like morphology were indeed glutamatergic juxtaglomerular neurons, we stained for the vesicular Glutamate Transporter 2 (vGluT2). This transmitter transporter is predominantly located at presynaptic vesicles as visualized by intense punctuate pattern in the immunostaining32. Accordingly, immunostaining is strongest in the afferent fibers of the sensory neurons arriving in the center of the glomeruli (Supplementary Figs. 4b, 5q,r,t,u). However, we also observed vGluT2-immunoreactive cell somata of virally traced GFP+ cells with a short-axon like morphology (Fig. 5b–d, i–l, n–q). While weak, this vGluT2-immunoreactivity was clearly specific, as neither juxtaglomerular cells with a different morphology (blue box in Fig. 5a,e–g) nor *GAD65*- or *GAD67*-expressing neurons exhibited this somatic vGluT2-immunoreactivity (Supplementary Fig. 5p–u). Notably, such cells were also reporter-positive 4 weeks after Tamoxifen-induction of *GLAST::CreERT2*25 mice crossed with the *R26R-CFP*33 reporter line (Supplementary Fig. 4b).

To further ensure the glutamatergic nature of the adult generated neurons, we combined *in-situ* hybridization to detect the cells synthesizing the vesicular glutamate transporters with

BrdU-labelling of adult generated cells. Intense *vGluT1* and *vGluT2* mRNA signals were observed in numerous cells located in the mitral cell layer, the external plexiform layer and the glomerular layer, but not in the GCL32, 34 (Fig. 6a-e; Supplementary Fig. 9a–c). Consistent with the glutamatergic nature of the *vGluT* mRNA-expressing cells in the glomerular layer, none was found to express *GAD67* driven GFP (data not shown and Supplementary Fig. 5p–u). As expected, many vGluT-expressing cells colocalized with Tbr1 or Tbr2, however a notable population of vGluT-expressing cells surrounding the glomeruli does not stain for Tbr1 or 2 (Supplementary Fig. 9d). Indeed, consistent the above observation that the adult generated progeny of Neurog2/Tbr2-expressing progenitors down-regulate Tbr proteins in the olfactory bulb, some adult born BrdU+ nuclei were framed by *vGluT2* mRNA (Fig. 6g) but BrdU/*vGluT2* mRNA expressing cells never colocalized with Tbr2 (Fig. 6h–j). BrdU seems not to label dying cells here as it was not observed in *vGluT2*+ cells shortly after BrdU-labelling (data not shown). Only after sufficient time to develop a transmitter phenotype, a small proportion of BrdU+ cells (2 ± 0.5%) located in the glomerular layer were found to express *vGluT2* (Supplementary Fig. 8e). Strikingly, none of the BrdU-labelled cells in the glomerular layer expressed *vGluT1* (1236 *vGluT1*+ cells analyzed; Fig. 6f), suggesting that only *vGluT2*-, but not *vGluT1*-expressing neurons are adult generated. Thus, three independent techniques labelling adult generated neurons support the generation of glutamatergic juxtaglomerular neurons in the adult olfactory bulb.

To assess the functional integration of the newly generated glutamatergic neurons, we immunostained for the immediate early gene c-fos known to be regulated by neuronal activity 3–6 weeks after BrdU administration35. c-fos immunoreactivity was detected in the majority of cells positive for both BrdU and *vGluT2* mRNA (86%, 60 cells, 3 animals; Fig. 6k,l) suggesting that most of the adult generated glutamatergic neurons become indeed functionally recruited about the same time as their GABAergic counterparts.

To further scrutinize the functional integration of these adult generated glutamatergic neurons we performed ultrastructural analysis in *E1- Neurog2/Cre Z/EG*-fate mapped cells in the glomerular layer stained for GFP with the electrondense DAB reaction product (Supplementary Fig. 10a). Cells with the morphology and at the position of the above described glutamatergic neurons were selected for electron microscopy and synapses formed by DAB-labelled processes were examined (Supplementary Fig. 10b). Consistent with previous evidence that vGluT-expression parallels the formation of asymmetric synapses in the olfactory bulb32, GFP+ pre-synaptic terminals established asymmetric contacts onto target cells in the glomerular layer (Supplementary Fig. 10c), confirming that juxtaglomerular neurons derived from Neurog2-positive precursors are excitatory and synaptically connected *in vivo*.

To examine the synapses formed by adult generated glutamatergic neurons at the physiological level, we used an *in vitro* system as the identification of the synaptic targets of a defined neuron by paired recordings in acute slices is virtually impossible. We took advantage of a previously established culture system of primary SEZ progenitors allowing for the maintenance of adult SEZ cells in the absence of mitogens under which condition they give rise predominantly to neuronal progeny thereby reflecting their endogenous lineage10. The majority of cells in this culture system are Dlx+10 as observed *in vivo* and in

agreement with their GABAergic fate. However, consistent with our *in vivo* observations, we also detected a small percentage of Tbr2+ cells (1.5%) (Fig. 7a,c) that could be transduced with a retroviral vector expressing GFP (Fig. 7c). Notably, the number of Tbr2+ cells increased when cells were isolated from the dorsal SEZ, while virtually no Tbr+ cells were contained in the lateral SEZ (Fig. 7b). Upon longer differentiation, a small proportion of cells exhibited vGluT- immunoreactivity which became concentrated in puncta after several weeks *in vitro* suggesting the formation of functional glutamatergic synapses (Fig. 7d,e; Supplementary Fig. 11a,b). When mature neurons were monitord by *synapsin* promoter driven GFP36, we found 3% (598 cells) to differentiate into a glutamamtergic (vGluT+) phenotype. To determine functional nature of glutamatergic synapses unambiguously we performed perforated patch recordings37 (Fig. 7e; Supplementary Fig. 11). When we used our observation that vGluT+ neurons possess relatively large cell somata, we found 9 out of 10 large *synapsin*-GFP+ cells (Fig. 7e; Supplementary Fig. 11) exhibited a CNQX-sensitive autaptic response (Figure 7e). Notably, neurons with such a response were indeed vGluT- immunopositive (Supplementary Fig. 11a,b). Furthermore, paired recordings demonstrated synaptically connected excitatory neurons in these cultures (Supplementary Fig. 11c) demonstrating that adult SEZ progenitors generate glutamatergic neurons forming functional synapses *in vitro*. Taken together, ultrastructural analysis, c-fos incorporation and *in vitro* physiology all support the physiologically relevant nature of glutamatergic olfactory neurons generated in the adult.

Tbr2+ cells migrate towards sites of neocortical injury

One of the implications of this discovery of endogenous glutamatergic progenitors in the adult SEZ is the possibility of their recruitment towards sites of neocortical injury. We therefore employed an injury model which has previously been shown to elicit remarkable repair of cortical projection neurons from endogenous sources of progenitors6, 7. Chlorine e_6-coupled beads were injected into the cortex to retrogradely label callosal projection neurons in the contralateral hemisphere7. Indeed, 7 days after injection, beads-containing neurons were observed in layers 2/3 and 5 of the contralateral site (Supplementary Fig. 12a). Subsequent (7 days after beads injection) laser illumination of the contralateral hemisphere allows activation of chlorine e_6 thus killing bead-containing neurons (as confirmed by staining for activated Caspase 3, Supplementary Fig. 12b). When we injected GFP encoding retroviral vectors into the adult SEZ 2 days prior to laser illumination, some of the transduced GFP+ cells migrating from the SEZ towards the lesion were Tbr2-immunoreactive (Fig. 8a). One week after laser exposure, clusters of Tbr2+/Dcx+ neuroblasts were found in the corpus callosum (Fig. 8b,c) and some had entered the cortical grey matter (Fig. 8d, n(animals)=3), while such invasion was never observed in control mice (n(animals)=4). Consistent with the lesion of callosal projection neurons, a fraction of $Tbr2^{BAC\text{-}GFP}$-positive cells were encountered in cortical layer 2 and 3 ten days after laser illumination. Accordingly, Foxp2-immunoreactivity (labelling lower cortical layers) was not detectable in these *Tbr2-GFP*+ cells (Supplementary Fig. 12d). In contrast, some of them were Cux1+ (Supplementary Fig. 12f) indicative of an upper layer neuron identity. Note the specificity of the staining as other cells at similar positions were still Cux1-immunonegative (Supplementary Fig. 12e). Of note, none of the adult generated neurons in the olfactory bulb

were Cux1+, suggesting that its expression in cells migrating into the injured cortex reflects the acquisition of a distinct glutamatergic subtype identity.

Taken together, these data suggest that at least some of the Tbr2+ cells in the SEZ and RMS serve as an endogenous source of progenitors that can be recruited to the cerebral cortex upon injury.

Discussion

Here we described for the first time the adult generation of glutamatergic juxtaglomerular neurons of the olfactory bulb. These glutamatergic neurons arise from a lineage that is characterized by the sequential expression of the transcription factors *Neurog2* → *Tbr2* → *Tbr1* that originates in the dorsal SEZ. These findings illustrate an unsuspected diversity of SEZ progenitors in regard to the transmitter phenotype of their progeny in the olfactory bulb that can be defined by their location in the dorsal SEZ and their combinatorial expression of different transcriptional cues.

Glutamatergic neurogenesis in the adult olfactory bulb

Thus far, the adult SEZ had been viewed as a region giving rise exclusively to GABAergic interneurons. Here we provide several independent lines of evidence that a subset of adult SEZ NSCs generates glutamatergic neurons. Firstly, we found that some BrdU-labelled cells in the glomerular layer express vGluT2, a transporter for glutamate into synaptic vesicles. Previous electron microscopic analysis in the adult olfactory bulb demonstrated that cells containing vGluT2 were exclusively neurons forming asymmetric excitatory synapses32, thereby supporting the glutamatergic identity of the cells examined here. Secondly, genetic and viral fate mapping shows that some adult generated neurons in the glomerular layer exhibit somatic immunoreactivity for vGluT2 protein32, consistent with the mRNA expression, identifying these neurons as glutamatergic. Thirdly, by genetic fate-mapping we demonstrate that BrdU+ neurons generated in the adult and derived from *Neurog2*-positive progenitors reach the glomerular layer and exhibit the morphology of short-axon cells. This notion is further confirmed at the ultrastructural level by the observation of asymmetric synaptic contacts established by the cells derived from the *Neurog2*-progenitor pool. Fourthly, consistent with the existence of adult NSCs generating glutamatergic neurons, we find a small proportion of glutamatergic neurons that form physiologically functional synapses *in vitro*. Thus, our *in vitro* and *in vivo* data unravelled a novel source for adult-generated glutamatergic neurons in the adult SEZ.

The genetic and viral fate mapping experiments permitted us to obtain more precise information on the morphology of the newly generated glutamatergic neurons in the glomerular layer. Very distinct from GABAergic periglomerular neurons (PGNs) these neurons typically extend their dendritic arbors adjoining several glomeruli characteristic of so called short-axon cells31, 38, a glutamatergic subpopulation of juxtaglomerular neurons. Of note, despite their small number short-axon cells play an important role as centre-surround inhibition among glomeruli by providing excitatory glutamatergic drive to inhibitory PGNs of up to 30 glomeruli31. However, we cannot exclude that other

subpopulations of juxtaglomerular glutamatergic neurons are also generated in the adult, potentially in a similar diversity of subtypes as observed for the GABAergic PGNs.

The physiological maturation and integration of these cells is supported by the expression of the immediate-early gene c-fos, a member of a family of transcription factors that are rapidly regulated by neuronal activity35. Detection of c-fos has previously been used to demonstrate integration of newborn neurons in the adult dentate gyrus39 and the olfactory bulb35. The expression of c-fos in the BrdU+/vGluT2+ neurons as well as the presence of asymmetric synaptic contacts established by Neurog2-derived neurons observed by electron microscopy therefore both support a functional integration of these newborn glutamatergic neurons into the neuronal network several weeks after their birth.

An exciting question is the functional role of this specific glutamatergic interneuron population. Indeed, even small subsets of olfactory neurons can have profound functional impact on olfactory information processing40 and the intriguing specificity of adult generation of vGluT2-expressing neurons in the glomerular layer prompts the suggestion that they perform a specific role in the glomerular layer neuronal network, the first synaptic station of the incoming afferents. Interestingly, synapses using vGluT2 for loading synaptic vesicles generally appear to exhibit a higher release probability compared to those expressing vGluT141. Given the pivotal role in centre-surround inhibition of short-axon cells it can be speculated that the new addition of glutamatergic neurons, like of their GABAergic counterparts, plays a crucial role in modifying the interglomerular circuitry during olfactory discrimination learning42.

SEZ regionalization and neuronal subtype specification

Recent evidence indicates that the SEZ in adult mice is highly regionalized, with stem cells in different locations having distinct embryonic origins and neuronal fates5, 13, 15, 16. In the present study we identify a novel SEZ progenitor population that is specifically localized in dorsal regions and undergoes the same transcription factor sequence that characterizes many glutamatergic subtypes throughout the brain12, 21. Sequential expression of Tbr2 and Tbr1 in developing neurons is a hallmark of glutamatergic lineage throughout the brain21. In the developing cerebral cortex and hippocampus, Tbr2-expressing progenitors arise from Neurog2-positive progenitors that themselves are generated by Pax6-expressing radial glia43.

Here we show that this transcription factor sequence is as well conserved in the adult dorsal SEZ (Supplementary Fig. 2, 13). While Pax6 is expressed in most Neurog2- or Tbr2-expressing cells, the latter never colocalized with Dlx. Interestingly, the Neurog2-expressing lineage originates also from Mash1-expressing progenitors as many Neurog2-positive cells in the RMS are also Mash1-positive (Supplementary Fig. 2c). Short-term fate mapping by *Mash1*$^{BAC\text{-}GFP}$ mice also revealed the origin of Tbr2+ progenitors from the Mash1-lineage (Supplementary Fig. 2d). This data imply that there are at least two different lineages arising from Pax6- and Mash1-expressing progenitors (Supplementary Fig. 13), a larger that leads to Pax6/Dlx-expressing neuroblasts and a smaller Pax6/Neurog2/Tbr2-expressing lineage (Supplementary Fig. 13). Thus, Pax6/Mash1-positive precursors can give rise to both GABA and glutamatergic lineages, raising the question of which signals regulate lineage

progression towards either of these. One candidate that might instruct dorsal SEZ progenitors towards a glutamatergic fate is beta catenin mediated Wnt-signaling, which is involved in up-regulation of Neurog1 via Lef1 that directly binds to the Neurog1 promotor *in vitro* in embryonic telencephalic progenitors44. Of note, Neurog1 and Neurog2 are typically expressed together20. Once Neurog2 is up-regulated, its functional relevance in the specification of glutamatergic neurons from adult SEZ cells is evident not only from developmental analysis20, 45 but also from the fact that over-expression of Neurog2 in adult-derived neurosphere cells is sufficient to up-regulate Tbr1 and to direct virtually all neurons towards a functional glutamatergic identity37.

A novel source for regenerating glutamatergic neurons

While neurogenesis in most regions of the telencephalon, including the striatum and cerebral cortex, ceases at early postnatal stages the ongoing olfactory neurogenesis serves as a potential source of neuroblasts after injury. Indeed, upon stroke many new neuroblasts migrate into the striatum and generate GABAergic neurons46. Surprisingly, neuroblasts from the SEZ and RMS also migrate into the cerebral cortex as observed after postnatal injury47, 48 or adult cerebral cortex lesion with Chlorine e_6-induced cell death6, 7. Using the latter model in conjunction with retroviral lineage tracing we could show that phototoxic lesion of the cerebral cortex results in re-routing of some SEZ progenitors out of the RMS towards the damaged cortex. Importantly some of the recruited SEZ progenitors expressed Tbr2 consistent with their derivation from the glutamatergic lineage. Upon settling in the damaged cortex some of these neurons appear to acquire the appropriate layer identity as suggested by expression of Cux1 in *Tbr*2-driven GFP+ cells in upper cortical layers following lesion of callosal projection neurons. In contrast, none of the adult generated glutamatergic neurons in the glomerular layer were found to express Cux1. This data therefore suggest that progenitors destined to generate glutamatergic juxtaglomerular neurons of the olfactory bulb, can be diverted towards a different, i.e. cortical projection neuron fate6, 7. While the molecular mechanisms underlying such re-specification remain unclear, they may involve local cues provided by the injured tissue. Notably, re-specification of SEZ-derived cells towards a different neuronal identity has been described with cells migrating after stroke from the SEZ into the striatum where they then acquire a Darp32-positive medium spiny neuronal phenotype that is normally not generated in the adult olfactory bulb neurogenesis46.

Taken together, the new discovery of ongoing generation of glutamatergic juxtaglomerular neurons highlights not only the exciting diversity of adult generated olfactory neurons in this region but also the importance of understanding the molecular code of the distinct subtypes of adult progenitors as a major step towards utilizing these neurons for repair. Indeed, the recent discovery of molecular fate determinants of subsets of cortical projection neurons may allow directing the novel source of adult progenitors for glutamatergic neurons identified here more efficiently towards the repair of cortical projection neurons.

Methods

Animals

All animal procedures were performed in accordance to the protocols approved by the state of Bavaria and in accordance with the UK (Scientific Procedures) animals's act 1986. For wild type analysis C57Bl6 mice were used in this study. In addition, the following knock-in mouse lines have been used: Mice with an eGFP cassette knocked-in the *Neurogenin2* locus (*Neurog2*$^{+/GFP}$)49 or *GAD67* locus (*GAD67::GFP*)28; or mice which express the Cre-recombinase in the *GLAST* locus25 crossed with the *R26R-CFP*33 reporter to follow recombined cells (*GLAST::CreERT2 R26R-CFP*). For induction of Cre-mediated recombination, animals were injected twice per day with 50 μl tamoxifen (20 mg/ml; dissolved in corn oil (Sigma)) for two times for 5 consecutive days with one week interval. We further used the transgenic mouse lines: BAC transgenics expressing GFP under the *Mash1* or *Tbr2* genomic regulatory sequences (*Mash1*$^{BAC\text{-}GFP}$, *Tbr2*$^{BAC\text{-}GFP}$)23, 50, and transgenic mice that express GFP under the *GAD65* promotor *GAD65-GFP*29 or mice expressing the Cre-recombinase under the enhancer-element 1 of Neurogenin230, 43 (*E1-Neurog2/Cre*) crossed with the Z/EG25 reporter (*E1-Neurog2/Cre Z/EG*) to follow the progeny derived of the Ngn2 derived lineage. All animals used in this study were adult with 2–3 months of age aside from the lentiviral ventricular injections where 3–4 weeks old mice were used.

BrdU treatment

For detection of proliferating cells, the DNA base analogue 5-Bromo-2′-deoxy-Uridine (BrdU, Sigma) was injected intraperitoneally (50–100 mg/kg body weight) one to two hours before perfusion to label fast proliferating cells (short pulse) or was given into drinking water for three weeks (1 mg/ml; complete exchange of water twice per week) followed by BrdU-free water for 3–4 weeks to allow full neuronal differentiation of labelled progenitors. For the BrdU chase experiment a single BrdU pulse was given to the pregnant mother at embryonic day E14 or postnatal day P3 (50 mg/kg body weight) and littermates were sacrificed at postnatal dayP16 and P60.

In-situ hybridization

The *vGluT1* and *vGluT2* plasmids used for *in-situ* hybridization were a kind gift of Dr. L. Cheng and Dr. Q. Ma. *Mash1* and *Neurog2* plasmids were provided by Dr. F. Guillemot, and the *Tbr2* and *GFP*24 were provided by Dr. R. Hevner and have been employed in previous studies; the *GAD65* and *GAD67* plasmids were obtained from Dr. W. Wurst.

Digoxigenin-labeled RNA probes were generated by *in vitro* transcription (NTP labelling mix, Roche and T3, T7 or SP6 polymerase, Stratagene) and *in-situ* hybridization was performed on 30 μm-thick cryostate sections or 70 μm-thick vibratome sections of perfused brains following standard protocols using α-Digoxigenin antibodies (Roche, 1:2000). For fluorescent *in-situ* hybridization a tyramide signal amplification kit (Perkin Elmer) was used.

Immunohistochemistry

For immunohistochemistry, animals were deeply anaesthetized using 5 % Chloralhydrate in PBS (0.1 ml/10 g bodyweight), transcardially perfused first with phosphate buffered saline (PBS) followed by 4 % paraformaldehyde (PFA) in PBS. Brains were dissected and post-fixed overnight in PFA at 4 °C. For cryostate sections, brains were cryoprotected, cut and immunostainings were carried out at 20 μm thickness. Alternatively, free-floating vibratome sections were cut at 60 μm thickness after post-fixation.

Primary antibodies were diluted in 0.1 M PBS containing 0.5 % Triton-X-100 and 10 % normal goat serum or 2 % Bovine Serum Albumin. We used primary antibodies to BrdU (rat, 1:400, Abcam or Accurate; sheep, 1:1000, Fitzgerald Industries); activated Caspase3 (Promega; rabbit, 1:200); c-fos (mouse, 1:200, Chemicon); pan-Dlx (1:500, Rabbit, kindly provided by J. Kohtz); doublecortin (Dcx, 1:2000, rabbit, Abcam or 1:500, goat, Santa Cruz); Gfap (1:250, guinea-pig, Advanced Immunochemical; 1:500, mouse, Chemicon); GFP (1:500, rabbit, Invitrogen, 1:1000 chicken, Abcam); Ki67 (goat, 1:500, Santa Cruz); Mash1 (mouse, 1:200, kindly provided by D. Anderson; mouse, 1:100, BD-Biosciences); Musashi (1:1000, rat, kindly provided by H Okano); Neurog2 (1:100, goat, Santa Cruz); Nestin (1:50, rabbit, Chemicon), Pax6 (mouse, 1:1000, kindly provided by D. Schulte, Developmental Studies Hybridoma Bank; rabbit, 1:300, Covance); PSA-NCAM (1:1000, mouse, Chemicon); Tbr1 (1:2000, rabbit, Chemicon or Abcam); Tbr2 (1:2000, rabbit, Chemicon or Abcam); vGluT1 (1:1000, rabbit, Synaptic Systems); vGluT2 (1:1000, rabbit Synaptic Systems). Specimens were incubated overnight at 4°C. After thorough washing, antibody stainings were revealed by appropriate species or subclass specific secondary antibodies conjugated to Alexa-488 (1:1000, Invitrogen), Alexa-568 (1:1000, Invitrogen), Cy2, Cy3 (1:1000, Dianova). Biotinylated secondary antibodies (1:200, Vector Laboratories) were used in combination with the TSA fluorescent amplification kit (Perkin Elmer). Specific labelling was checked by omitting the primary antibody.

BrdU immunohistochemistry was performed as described above after 2 M HCl pre-treatment for 45 – 60 min followed by incubation in borate buffer (0.1 M, 10 minutes, pH 8.5). Antigen retrieval for detection of Neurog2 protein was done using citrate buffer (0.1 M, pH 6, 20 minutes, 80 °C).

Viral vector injections

The retro- or lentiviral vector used in this study encoded only for GFP, driven by a CAG promoter or ubiquitin promoter, respectively. Viral preparations and injections were performed as described previously10, 13. Briefly, mice were deeply anesthetized (ketamine (100 mg/kg; CP-Pharma) and xylazine (5 mg/kg; Rompun; Bayer)) and injected with 0.5 μl of viral suspension at the following coordinates (relative to bregma): for adult SEZ, 0.7 (anteroposterior), 1.2 (mediolateral), and 1.7–1.4 (dorsoventral); and for ventricular injections at the age of 3 weeks, on the level of bregma 0.8 (mediolateral), and −2.0 (dorsoventral).

Immunoelectron microscopy

For electron microscopic analysis, animals were perfused with 4 % PFA containing 0.1 % glutaraldehyde and post-fixed over night at 4 °C. Free-floating vibratome sections of 50 μm thickness were incubated in primary antibody over night at 4 °C. After thorough washing, staining for electron microscopic analysis were detected by a biotin-conjugated secondary antibody (1:200, Vector labs), followed by the ABC kit (Vector labs) and DAB (Polysciences) labelling. The intensity of the staining reaction was monitored in the microscope. Control sections were stained with the secondary antibody alone, where no staining could be observed. Sections containing DAB-stained cells were dehydrated in ascending series of ethanol and finally embedded in Durcupan. Ultrathin sections were cut on a Reichert Ultratome and viewed in a Philips 100 Electron Microscope.

Statistical analysis

Stainings were analyzed at an Olympus FV1000, a Leica SPE or Zeiss LSM5 Pascal laser-scanning confocal microscope with optical sections of maximum 1–1.5 μm intervals or with Zeiss AxioImager.Z1 with apotome component. Colocalization with cell type specific antigens was quantified in single optical sections of the laser-scanning microscopes. Between 5 and 10 sections per animal were counted per experiment until comparable numbers of stained or GFP+ cells per animal or experiment was reached. The total number of cells counted in all animals is indicated in the text. One animal or experiment represents one mean value and standard deviations were calculated between animals or cultures. All error bars are presented as standard errors of the mean (± s. e. m.). For the 3D-reconstruction of the location *of Neurog2*$^{+/GFP}$-positive and Tbr2+ cells and of the dendritic arborization of *E1- Neurog2/Cre Z/EG* fate-mapped cells the Neurolucida software was used.

Cultures and electrophysiology

Primary cultures of adult SEZ stem and progenitor cells were prepared as described previously10. In brief, following dissection of the SEZ of adult mice (> 8 weeks), cells were directly plated onto poly-D-lysine coated cover slips in defined medium containing DMEM/F12 (Gibco), 10 mM HEPES (Gibco), supplemented with B27 (Gibco) in the absence of epidermal growth factor (EGF) and fibroblast growth factor 2 (FGF2). Dorsal SEZ cultures were obtained by dissecting the upper third of the whole ventricular wall including the white matter, whereas the lower two third of the ventricular wall were referred to as lateral SEZ cultures. For retroviral labelling cultures were transduced 2 hours after plating. Two days after plating 50 % of the medium was replaced by fresh medium and cells were subsequently maintained for the indicated time periods until electrophysiological analysis or fixation for immunocytochemistry.

For electrophysiology, perforated patch-clamp recordings were performed at room temperature with amphotericin-B (Calbiochem) for perforation37. Micropipettes were made from borosilicate glass capillaries. Pipettes were tip-filled with internal solution and backfilled with internal solution containing 200 μg/ml amphotericin-B. The electrodes had resistances of 2–2.5 MΩ. The internal solution contained 136.5 mM K-gluconate, 17.5 mM KCl, 9 mM NaCl, 1 mM $MgCl_2$, 10 mM HEPES, 0.2 mM EGTA (pH 7.4) at an osmolarity of 300 mOsm. The external solution contained 150 mM NaCl, 3 mM KCl, 3 mM $CaCl_2$, 2

mM $MgCl_2$, 10 mM HEPES, 5 mM glucose (pH 7.4) at an osmolarity of 310 mOsm. The recording chamber was continuously perfused with external solution at a rate of 0.5 ml/min. Cells were visualized with a Zeiss Axioskop2. Signals were sampled at 10 kHz with Axopatch 200B patch-clamp amplifiers (Axon instruments), filtered at 5 kHz and analyzed with Clampfit 9.2 software (Axon Instruments). In order to assess autaptic connections, single cells were step-depolarized in voltage clamp for 1 ms from −70 to + 30 mV and responses were recorded in the same cell. Responses were considered to be autaptic when they occurred within 3 ms after the step-depolarization. To visualize neurons for electrophysiology, adult SEZ cultures were transduced 14 days after plating with a lentiviral SYN-SYN-GFP vector36, encoding GFP under the control of the *human synapsin* promoter which allows specific labelling of neurons.

Chlorine e_6 induced cortical lesion

Chlorine e_6 (Frontier Scientific) was coupled to latex beads (Lumaflour) as reported previously6, 7. Briefly, 3 ml of 0.01 M phosphate buffer (PB, pH 7.4), were used to dissolve 1.79 mg Chlorine e_6 and 5 mg of 1-ethyl-3-(3-dimethylaminopropyl)-carbodiimide (MP Biomedicals) was added. The solution was kept for 30 minutes at 4 °C. 25 μl of rhodamine latex beads (Lumafluor) were incubated on a shaker for 1 hour at room temperature with 1.5 ml of activated Chlorine e_6 solution. The reaction was stopped by adding 200 μl of 0.1 M glycine buffer (pH 8.0). The coupled latex beads were centrifuged to remove the supernatant (30 minutes, 50.000 g), washed at least three times with 10 ml 0.01 M PB, re-suspended in about 50 μl 0.01 M PB, and stored at 4 °C. Injections were performed 5–7 times into the cerebral cortex (maximum depth 0.8 mm, around 100 nl each injection) by the use of a glass capillary connected with an air pressure system (WPI). Retrograde transport of latex beads was checked in control animals that did not undergo laser illumination. Laser illumination (633nm; Schafter and Kirchhoff) of the contra-lateral hemisphere was performed directly on the dura after skull removement 2, 3, or 7 days later (5 minutes) followed by transcardial perfusion 7 or 10 days later. Different illumination times (20, 10, 5, 2 minutes) and different laser intensities (100, 50, 20, 10, 5 mW) were tested and best results (number and specificity of dying cells) were obtained with 20–30 mW for 4–5 minutes. For the tracking experiments, retroviral injections were performed in one hemisphere, parallel with Chlorine e_6 coupled latexbeads on the contralateral side, followed by laser illumination 2 days later, and perfusion 3–4 days later. Cell death was confirmed by staining for active Caspase 3 and NeuN 3 days after laser illumination on the contralateral hemisphere.

Supplementary Material

Refer to Web version on PubMed Central for supplementary material.

Acknowledgments

We would like to thank Francesco Bedogni for invaluable advice on methods and we are particularly grateful for the GAD67::GFP mice to Dr. Yuchio Yanagawa. We would also like to thank Tatiana Simon-Ebert, Andrea Steiner, Timucin Öztürk, and Sigrun Nestel for excellent technical assistance and Simone Bauer for retroviral production. This work was supported by grants of the DFG including the excellence cluster CIPSM, by EUTRACC from the EU and the BMBF to M. G. and the Bavarian State Ministry of Sciences, Research, and the Arts (ForNeuroCell) to B. B. and M. G.. E. W. is supported by a fellowship from the MRC, I. O. by a fellowship from the John & Lucille van Geest Foundation, and O. R by a grant from the Dr Scholl Foundation. Research in the

laboratory of F. G. is supported by funds from the Medical Research Council and grants from the European Commission Research and Technological Development program. C. P. is presently supported by an AVENIR Contract from INSERM and Fondation de France. R. D. H. is supported by a Heart and Stroke Fund of Canada Research Fellowship. Work done in the laboratory of R. F. H. was supported by grants from the National Institutes of Health (R01 NS050248, R01 MH080766).

References

1. Kokaia Z, Lindvall O. Neurogenesis after ischaemic brain insults. Curr Opin Neurobiol. 2003; 13:127–32. [PubMed: 12593991]
2. Sohur US, Emsley JG, Mitchell BD, Macklis JD. Adult neurogenesis and cellular brain repair with neural progenitors, precursors and stem cells. Philos Trans R Soc Lond B Biol Sci. 2006; 361:1477–97. [PubMed: 16939970]
3. Ming GL, Song H. Adult neurogenesis in the mammalian central nervous system. Annu Rev Neurosci. 2005; 28:223–50. [PubMed: 16022595]
4. Gage FH. Mammalian neural stem cells. Science. 2000; 287:1433–8. [PubMed: 10688783]
5. Merkle FT, Mirzadeh Z, Alvarez-Buylla A. Mosaic organization of neural stem cells in the adult brain. Science. 2007; 317:381–4. [PubMed: 17615304]
6. Chen J, Magavi SS, Macklis JD. Neurogenesis of corticospinal motor neurons extending spinal projections in adult mice. Proc Natl Acad Sci U S A. 2004; 101:16357–62. [PubMed: 15534207]
7. Magavi SS, Leavitt BR, Macklis JD. Induction of neurogenesis in the neocortex of adult mice. 2000; 405:951–955.
8. Lledo PM, Alonso M, Grubb MS. Adult neurogenesis and functional plasticity in neuronal circuits. Nat Rev Neurosci. 2006; 7:179–93. [PubMed: 16495940]
9. Wonders CP, Anderson SA. The origin and specification of cortical interneurons. Nat Rev Neurosci. 2006; 7:687–96. [PubMed: 16883309]
10. Brill MS, et al. A dlx2- and pax6-dependent transcriptional code for periglomerular neuron specification in the adult olfactory bulb. J Neurosci. 2008; 28:6439–52. [PubMed: 18562615]
11. Waclaw RR, et al. The zinc finger transcription factor Sp8 regulates the generation and diversity of olfactory bulb interneurons. Neuron. 2006; 49:503–16. [PubMed: 16476661]
12. Bertrand N, Castro DS, Guillemot F. Proneural genes and the specification of neural cell types. Nat Rev Neurosci. 2002; 3:517–30. [PubMed: 12094208]
13. Hack MA, et al. Neuronal fate determinants of adult olfactory bulb neurogenesis. Nat Neurosci. 2005; 8:865–72. [PubMed: 15951811]
14. Roybon L, Deierborg T, Brundin P, Li JY. Involvement of Ngn2, Tbr and NeuroD proteins during postnatal olfactory bulb neurogenesis. Eur J Neurosci. 2009; 29:232–43. [PubMed: 19200230]
15. Young KM, Fogarty M, Kessaris N, Richardson WD. Subventricular zone stem cells are heterogeneous with respect to their embryonic origins and neurogenic fates in the adult olfactory bulb. J Neurosci. 2007; 27:8286–96. [PubMed: 17670975]
16. Kohwi M, et al. A subpopulation of olfactory bulb GABAergic interneurons is derived from Emx1- and Dlx5/6-expressing progenitors. J Neurosci. 2007; 27:6878–91. [PubMed: 17596436]
17. Kroll TT, O'Leary DD. Ventralized dorsal telencephalic progenitors in Pax6 mutant mice generate GABA interneurons of a lateral ganglionic eminence fate. Proc Natl Acad Sci U S A. 2005; 102:7374–9. [PubMed: 15878992]
18. Nikoletopoulou V, et al. Neurotrophin Receptor-Mediated Death of Misspecified Neurons Generated from Embryonic Stem Cells Lacking Pax6. Cell Stem Cell. 2007; 1:529–540. [PubMed: 18371392]
19. Dellovade TL, Pfaff DW, Schwanzel-Fukuda M. Olfactory bulb development is altered in small-eye (Sey) mice. J Comp Neurol. 1998; 402:402–18. [PubMed: 9853907]
20. Schuurmans C, et al. Sequential phases of cortical specification involve Neurogenin-dependent and -independent pathways. Embo J. 2004; 23:2892–902. [PubMed: 15229646]
21. Hevner RF, Hodge RD, Daza RA, Englund C. Transcription factors in glutamatergic neurogenesis: conserved programs in neocortex, cerebellum, and adult hippocampus. Neurosci Res. 2006; 55:223–33. [PubMed: 16621079]

22. Hevner RF, et al. Tbr1 regulates differentiation of the preplate and layer 6. Neuron. 2001; 29:353–66. [PubMed: 11239428]
23. Geschwind D. GENSAT: a genomic resource for neuroscience research. Lancet Neurol. 2004; 3:82. [PubMed: 14746997]
24. Kowalczyk T, et al. Intermediate Neuronal Progenitors (Basal Progenitors) Produce Pyramidal-Projection Neurons for All Layers of Cerebral Cortex. Cereb Cortex. 2009
25. Ninkovic J, Mori T, Gotz M. Distinct modes of neuron addition in adult mouse neurogenesis. J Neurosci. 2007; 27:10906–11. [PubMed: 17913924]
26. Mori T, et al. Inducible gene deletion in astroglia and radial glia--a valuable tool for functional and lineage analysis. Glia. 2006; 54:21–34. [PubMed: 16652340]
27. Liu X, Wang Q, Haydar TF, Bordey A. Nonsynaptic GABA signaling in postnatal subventricular zone controls proliferation of GFAP-expressing progenitors. Nat Neurosci. 2005; 8:1179–87. [PubMed: 16116450]
28. Tamamaki N, et al. Green fluorescent protein expression and colocalization with calretinin, parvalbumin, and somatostatin in the GAD67-GFP knock-in mouse. J Comp Neurol. 2003; 467:60–79. [PubMed: 14574680]
29. Lopez-Bendito G, et al. Preferential origin and layer destination of GAD65-GFP cortical interneurons. Cereb Cortex. 2004; 14:1122–33. [PubMed: 15115742]
30. Berger J, et al. E1-Ngn2/Cre is a new line for regional activation of Cre recombinase in the developing CNS. Genesis. 2004; 40:195–9. [PubMed: 15593326]
31. Aungst JL, et al. Centre-surround inhibition among olfactory bulb glomeruli. Nature. 2003; 426:623–9. [PubMed: 14668854]
32. Gabellec MM, Panzanelli P, Sassoe-Pognetto M, Lledo PM. Synapse-specific localization of vesicular glutamate transporters in the rat olfactory bulb. Eur J Neurosci. 2007; 25:1373–83. [PubMed: 17425564]
33. Srinivas S, et al. Cre reporter strains produced by targeted insertion of EYFP and ECFP into the ROSA26 locus. BMC Dev Biol. 2001; 1:4. [PubMed: 11299042]
34. Ohmomo H, et al. Postnatal changes in expression of vesicular glutamate transporters in the main olfactory bulb of the rat. Neuroscience. 2009; 160:419–26. [PubMed: 19264112]
35. Magavi SS, Mitchell BD, Szentirmai O, Carter BS, Macklis JD. Adult-born and preexisting olfactory granule neurons undergo distinct experience-dependent modifications of their olfactory responses in vivo. J Neurosci. 2005; 25:10729–39. [PubMed: 16291946]
36. Gascon S, Paez-Gomez JA, Diaz-Guerra M, Scheiffele P, Scholl FG. Dual-promoter lentiviral vectors for constitutive and regulated gene expression in neurons. J Neurosci Methods. 2008; 168:104–12. [PubMed: 17983662]
37. Berninger B, Guillemot F, Gotz M. Directing neurotransmitter identity of neurones derived from expanded adult neural stem cells. Eur J Neurosci. 2007; 25:2581–90. [PubMed: 17561834]
38. Pinching AJ, Powell TP. The neuron types of the glomerular layer of the olfactory bulb. J Cell Sci. 1971; 9:305–45. [PubMed: 4108056]
39. Jessberger S, et al. Seizure-associated, aberrant neurogenesis in adult rats characterized with retrovirus-mediated cell labeling. J Neurosci. 2007; 27:9400–7. [PubMed: 17728453]
40. Eyre MD, Kerti K, Nusser Z. Molecular diversity of deep short-axon cells of the rat main olfactory bulb. Eur J Neurosci. 2009; 29:1397–407. [PubMed: 19344330]
41. Murphy GJ, Isaacson JS. Presynaptic cyclic nucleotide-gated ion channels modulate neurotransmission in the mammalian olfactory bulb. Neuron. 2003; 37:639–47. [PubMed: 12597861]
42. Mouret A, et al. Learning and survival of newly generated neurons: when time matters. J Neurosci. 2008; 28:11511–6. [PubMed: 18987187]
43. Scardigli R, Baumer N, Gruss P, Guillemot F, Le Roux I. Direct and concentration-dependent regulation of the proneural gene Neurogenin2 by Pax6. Development. 2003; 130:3269–81. [PubMed: 12783797]

44. Israsena N, Hu M, Fu W, Kan L, Kessler JA. The presence of FGF2 signaling determines whether beta-catenin exerts effects on proliferation or neuronal differentiation of neural stem cells. Dev Biol. 2004; 268:220–31. [PubMed: 15031118]

45. Parras CM, et al. Divergent functions of the proneural genes Mash1 and Ngn2 in the specification of neuronal subtype identity. Genes Dev. 2002; 16:324–38. [PubMed: 11825874]

46. Arvidsson A, Collin T, Kirik D, Kokaia Z, Lindvall O. Neuronal replacement from endogenous precursors in the adult brain after stroke. Nat Med. 2002; 8:963–70. [PubMed: 12161747]

47. Goings GE, Sahni V, Szele FG. Migration patterns of subventricular zone cells in adult mice change after cerebral cortex injury. Brain Res. 2004; 996:213–26. [PubMed: 14697499]

48. Faiz M, et al. Substantial migration of SVZ cells to the cortex results in the generation of new neurons in the excitotoxically damaged immature rat brain. Mol Cell Neurosci. 2008; 38:170–82. [PubMed: 18434192]

49. Seibt J, et al. Neurogenin2 specifies the connectivity of thalamic neurons by controlling axon responsiveness to intermediate target cues. Neuron. 2003; 39:439–52. [PubMed: 12895419]

50. Parras CM, et al. Mash1 specifies neurons and oligodendrocytes in the postnatal brain. Embo J. 2004; 23:4495–505. [PubMed: 15496983]

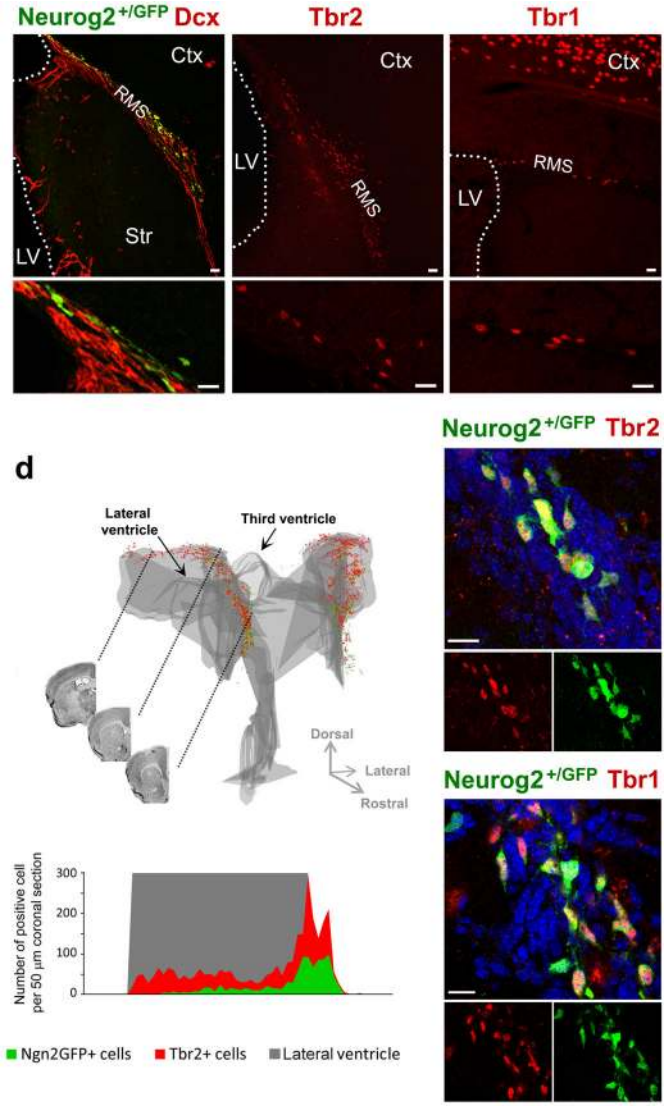

Figure 1. *Neurog2*$^{+/GFP}$ and Tbr1m&2 are expressed in a defined, dorsal region of the SEZ

(**a–c**) Fluorescent micrographs depicting *Neurog2*$^{+/GFP}$-, Tbr2- and Tbr1-positive cells as indicated in the panels in the dorsal SEZ and RMS.

(**d**) 3D-reconstruction of the localization of *Neurog2*$^{+/GFP}$- (green) and Tbr2-positive (red) cells in the adult forebrain shows that these progenitors are located in the dorsal SEZ, but not in the lateral wall of the lateral ventricle or third ventricle. Coronal views of three different levels are indicated by the black lines. The histogram below depicts the distribution of *Neurog2*$^{+/GFP}$- and Tbr2-positive cells along the rostro-caudal axis. Note that Tbr2-positive cells are more widespread than *Neurog2*$^{+/GFP}$-positive cells and that the expression of both markers drops rapidly upon entrance of the cells into the RMS. (**e–f**) *Neurog2*$^{+/GFP}$ cells are immunoreactive for (**e**) Tbr2 and (**f**) Tbr1.

Nuclei are visualized with DAPI (**e,f**). Ctx = Cortex, LV = lateral ventricle, RMS = rostral migratory stream, Str = Striatum, scale bars: 20 µm.

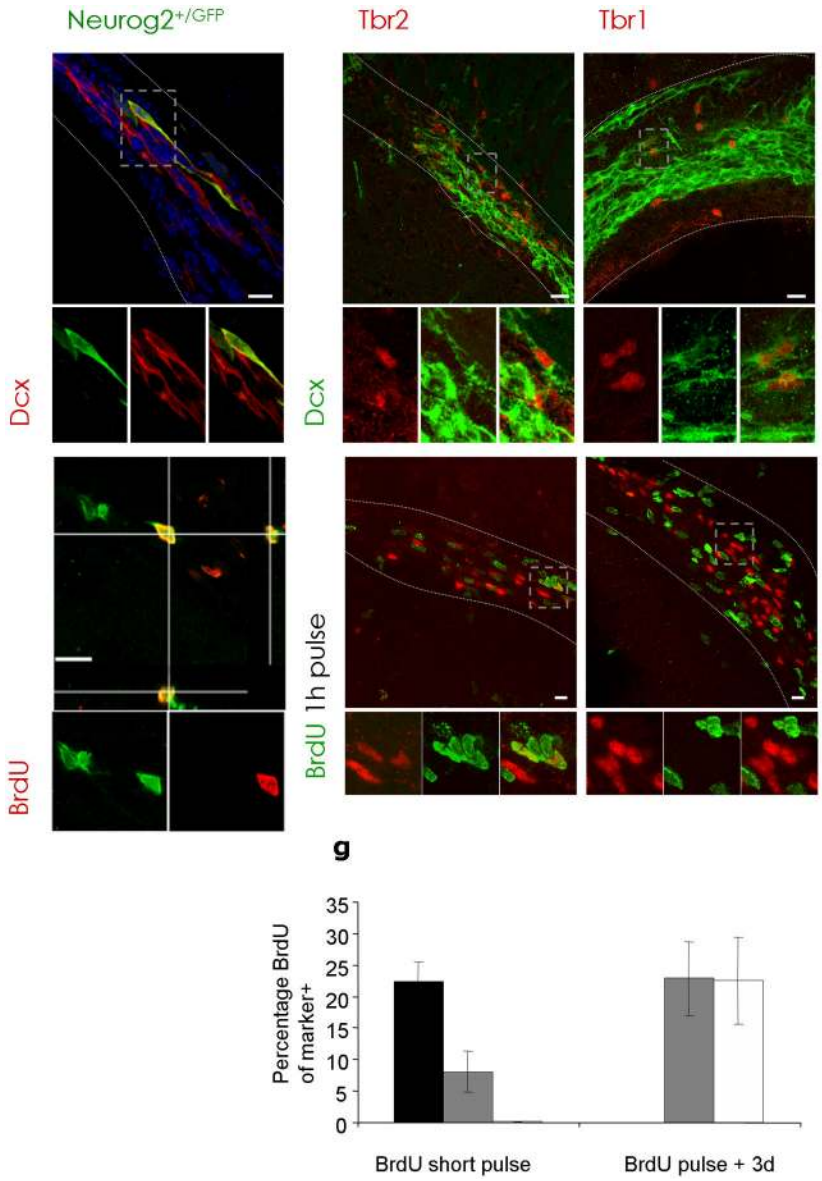

Figure 2. Neurog2, Tbr1 and Tbr2 expression defines a subset of neuroblasts

(**a–c**) Fluorescent micrographs depicting *Neurog2*$^{+/GFP}$-, Tbr2-, and Tbr1-staining in a subpopulation of Dcx-positive neuroblasts in the RMS and dorsal SEZ; (**d–e**) depict *Neurog2*$^{+/GFP}$- and Tbr2-positive cells labelled with BrdU after a short BrdU pulse, while Tbr1-positive cells (**f**) are not BrdU-positive. Boxed areas (grey) are shown at higher magnification at the bottom of the panels. (**g**) Histogram depicting the proportion of *Neurog2*$^{+/GFP}$-, Tbr2- and Tbr*1*-expressing cells in the RMS labelled with BrdU as indicated. Both, Tbr2 and *Neurog2*$^{+/GFP}$ are detected in fast proliferating cells, while Tbr1-positive cells are labelled only 3 days after BrdU application. (n = 3 animals; cells *Neurog2*$^{+/GFP}$, short pulse = 116, cells Tbr1, short pulse = 144, cells Tbr1, 3 days = 190; cells Tbr2, short pulse = 285, cells Tbr2, 3 days = 166). Error bars are presented as s. e. m. dSEZ = dorsal subependymal zone, LV = lateral ventricle, RMS = rostral migratory stream, Str = Striatum, WM = white matter, scalebars: 20 μm.

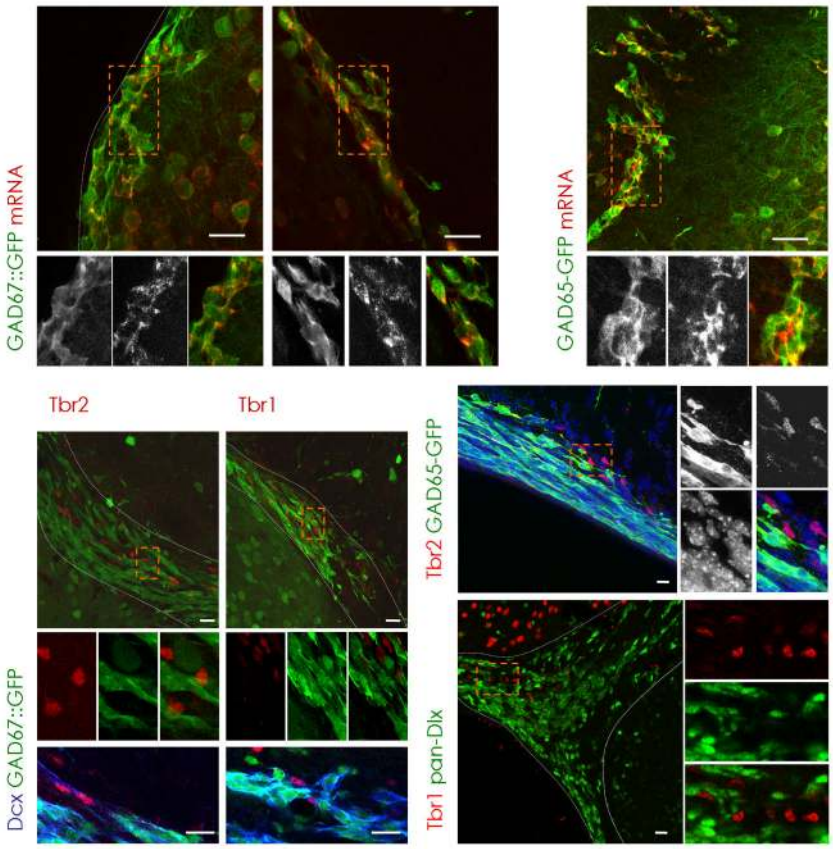

Figure 3. Presence of Tbr2 and Tbr1 defines a non-GABAergic subpopulation of neuroblasts

(**a–c**) Virtually all GFP-positive cells in the SEZ (**a,c**) and RMS (**b**) are colocalizing with *GAD67* (**a,b**) or *GAD65* (**c**) mRNA in the respective *GAD67::GFP* and *GAD65-GFP* mouse lines as indicated in the panels (see Methods). Notably, Tbr2 (**d,h**) and Tbr1 (**e**) are absent in *GAD65*- (**h**) or *GAD67*- (**d–g**) driven GFP-positive cells, but are immunoreactive for the neuroblast marker Dcx in the dorsal SEZ (Tbr2, **f**) and RMS (Tbr1, **g**). (**i**) Consistently, Dlx transcription factors (pan-*Dlx*, green) are not coexpressed with Tbr1 (red). (**a–e,h,i**) Boxed areas (orange) are shown at higher magnification. Nuclei are visualized with DAPI (**h**). dSEZ = dorsal subependymal zone, LV = lateral ventricle, RMS = rostral migratory stream, SEZ = subependymal zone, Str = Striatum, WM = white matter, latSEZ = lateral subependymal zone, scale bars: 20 μm.

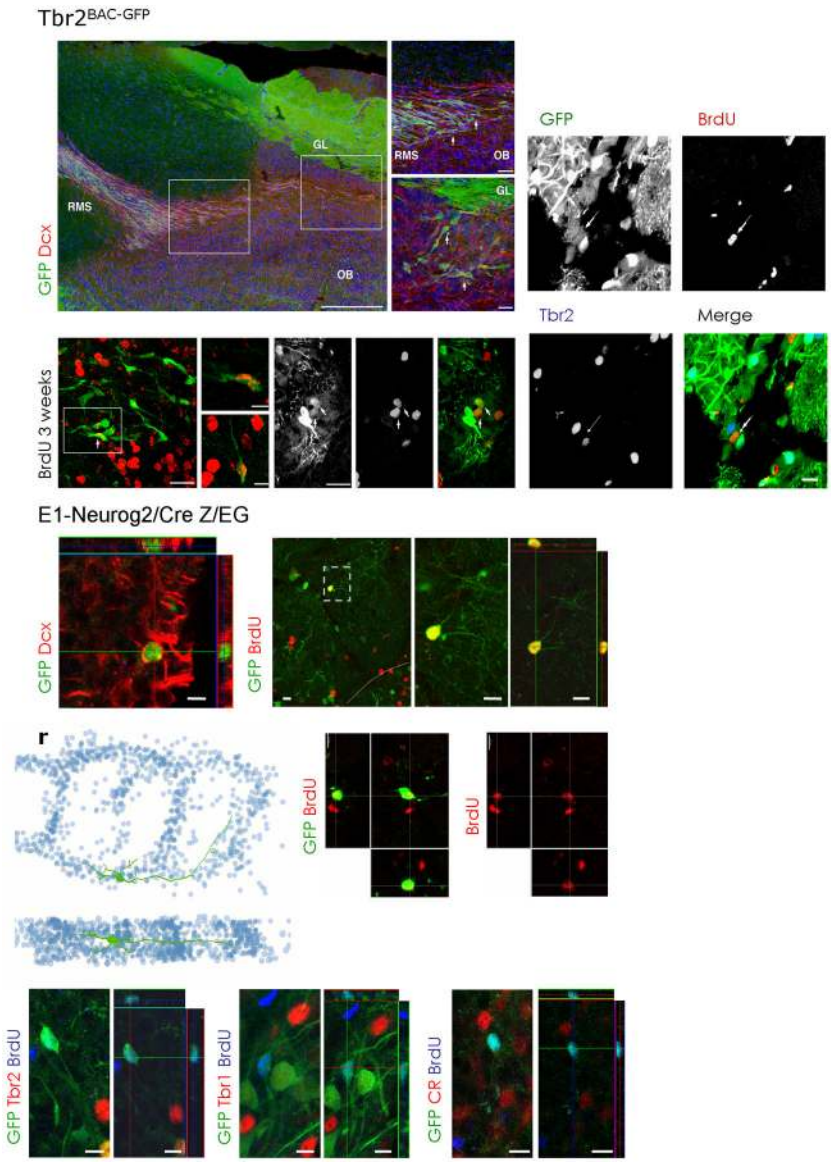

Figure 4. Fate mapping of Tbr2- or Neurog2-derived progeny in the olfactory bulb

(**a–c**) Fluorescent micrographs depicting *Tbr2*$^{BAC\text{-}GFP}$-positive cells in the RMS and olfactory bulb (green) and Dcx-positive neuroblasts (red). Boxed areas (white) are shown in higher magnifications in (**b,c**) depicting cells in the RMS entering the olfactory bulb (OB) (**b**) and on their way to the glomerular layer (GL) (**c**).

(**d–i**) Fluorescent micrographs depicting examples of BrdU-labelled *Tbr2*$^{BAC\text{-}GFP}$-positive cells (arrows) that are apparent in the glomerular layer of the olfactory bulb 3 weeks after BrdU labelling. (**j–m**) Consistently, the BrdU/*Tbr2*$^{BAC\text{-}GFP}$ fate-mapped cells (example indicated by arrow) were negative for Tbr2 protein.

Fate mapping of Neurog2 derived progeny in the glomerular layer (GL) of the olfactory bulb using *E1- Neurog2/Cre Z/EG* mice (**n**) shows the presence of GFP-positive neuroblasts (Dcx, red). (**o–q**) BrdU labels juxtaglomerular cells expressing GFP derived from Neurog2 expression (*E1- Neurog2/Cre Z/EG*). BrdU was given 3 weeks drinking water followed by a

3 weeks BrdU-free period. Boxed area (gey) is shown at higher magnification as (**p**) Z-projection and (**q**) as single optical section.

(**r–t**) 3D-reconstruction of the dendritic arborization of a *Neurog2*-derived adult labelled GFP/BrdU double-positive cell. (**s,t**) The reconstructed cell is derived from serial sections of a cell labelled for GFP by *E1- Neurog2/Cre Z/EG* fate mapping and for adult generation by BrdU incorporation (red). BrdU was given for 3 weeks into the drinking water followed by 3 weeks BrdU-free water.

(**u–z**) Note that adult born *Neurog2* derived GFP-positive cells that had incorporated BrdU (blue) are negative for Tbr2 (red) (**u,v**), Tbr1 (red) (**w,x**) or calretinin (CR, red) (**y,z**). (**u,w,y**) are Z-projections, (**v,x,z**) are single optical sections.

EPL = external plexiform layer, GL = glomerular layer, OB = olfactory bulb, RMS = rostral migratory stream, scale bars: 20 μm.

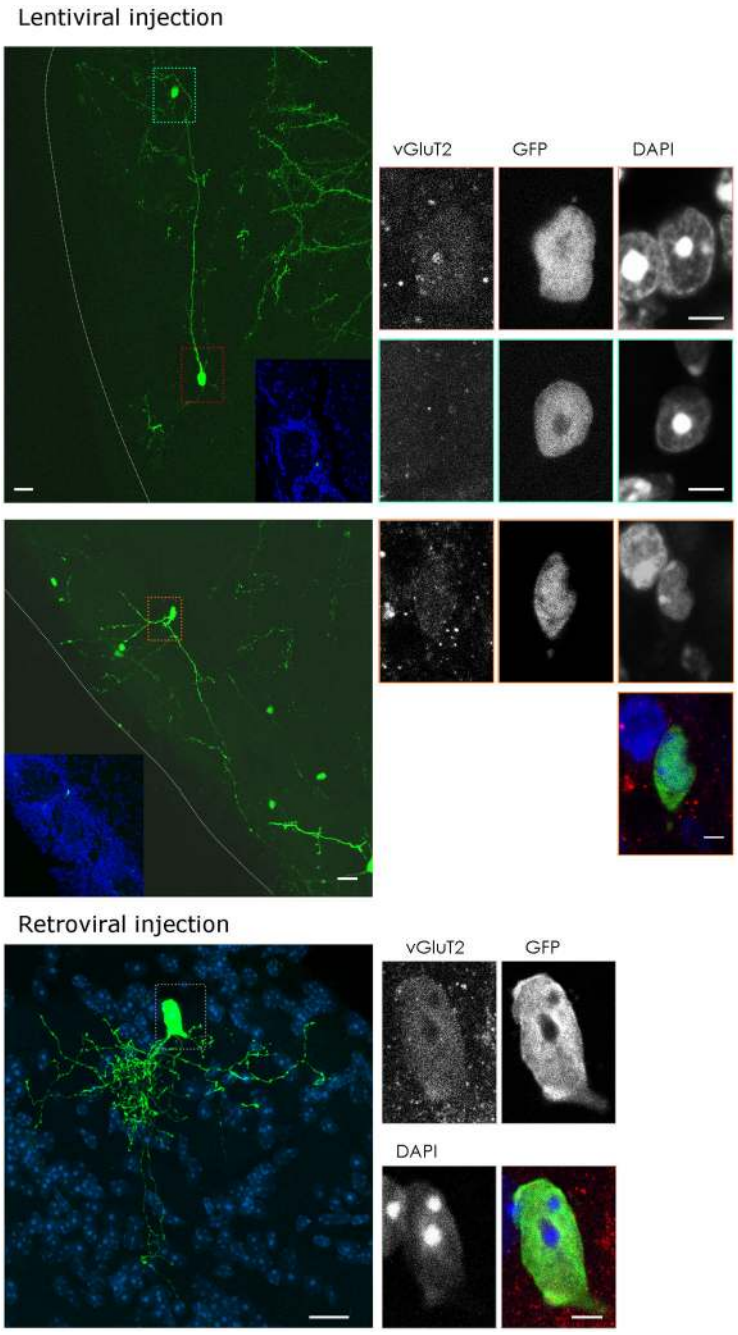

Figure 5. Viral vector mediated fate mapping of vGluT2-expressing juxtaglomerular neurons

(**a–i**) GFP encoding lentivirus injections into the murine ventricle at the age of 3 weeks resulted in numerous GFP-positive cells in the glomerular layer of the olfactory bulb 6 weeks later. Some GFP-expressing cells had vGluT2-immunoreactivity in their soma ((**b–d**); red box in (**a**); (**i–l**), orange box in (**h**)), while the majority of GFP-expressing transduced cells were negative for somatic vGluT2-immunoreactivity ((**e–g**); green-blue box in (**a**)). (**m–q**) Retroviral vector injection into dorsal regions of the adult SEZ analyzed 6 weeks post injection also resulted in some GFP-positive juxtaglomerular neurons with somatic vGluT2 (red) immunoreactivity shown in (**n–q**). Nuclei are visualized with DAPI (**d,g,k,l,m,p,q**).

Insets in (**a,h**) show an overview of the juxtaglomerular location of the GFP-labelled neurons by counterstaining with DAPI visualizing the glomeruli. (**b–g, i–l, n–q**) are single optical sections, whereas (**a,h,m**) are collapsed stacks to show the morphology vGluT2-immunoreactive juxtaglomerular cells.

GL = glomerular layer, EPL = external plexiform layer, scale bars: (**a,h,m**) 20 μm, (**b–g, i–l, n–q**) 5 μm.

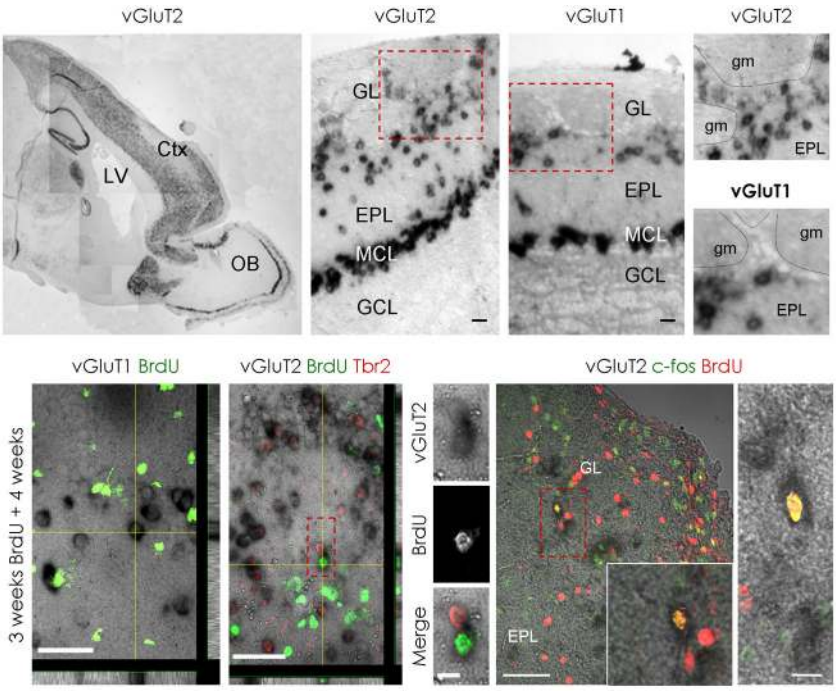

Figure 6. A subpopulation of newly generated juxtaglomerular neurons expresses *vGluT2* mRNA

In-situ hybridization for the vesicular glutamate transporter 2 (*vGluT2*) (**a,b,d**) or *vGluT1* (**c,e**) mRNA in the adult olfactory bulb shows expression in the mitral cell layer (MCL), external plexiform layer (EPL) and glomerular layer (GL). In contrast, no mRNA signal for *vGluT1* nor *vGluT2* was detected in the granule cell layer (GCL) (**a-c**). Boxed areas (red) are shown at higher magnification in (**d,e**). Note that only *vGluT2* mRNA is detected between glomeruli (gm) whereas *vGluT1* mRNA is largely restricted to the external plexiform layer underlying the glomerular layer. (**f**) depicts a micrograph with BrdU-immunofluorescence in green and *vGluT1* mRNA in black. Note that *vGluT1*-expressing cells do not incorporate BrdU. (**g**) depicts an example of *vGluT2*-expressing juxtaglomerular cell labelled by BrdU (green) that is Tbr2-negative (red). Boxed area (red) is shown in higher magnification in (**h–j**). (**k,l**) depict two examples of *vGluT2*-expressing cells that incorporated BrdU (red) and are immunopositive for c-fos (green). Boxed area in (**k**) (red) is shown at higher magnification at the lower right corner of the panel. Z-projections in (**f**) and (**g**) are shown below and to the right of the panels.

Ctx = Cortex, GL = glomerular layer, EPL = external plexiform layer, LV = lateral ventricle, MCL = mitral cell layer, GCL = granule cell layer, gm = glomerulus, OB = olfactory bulb, scale bars: (**b,c,l**) 20 μm, (**h–j**) 10 μm, (**f,g**) 50μm, (**k**) 100 μm.

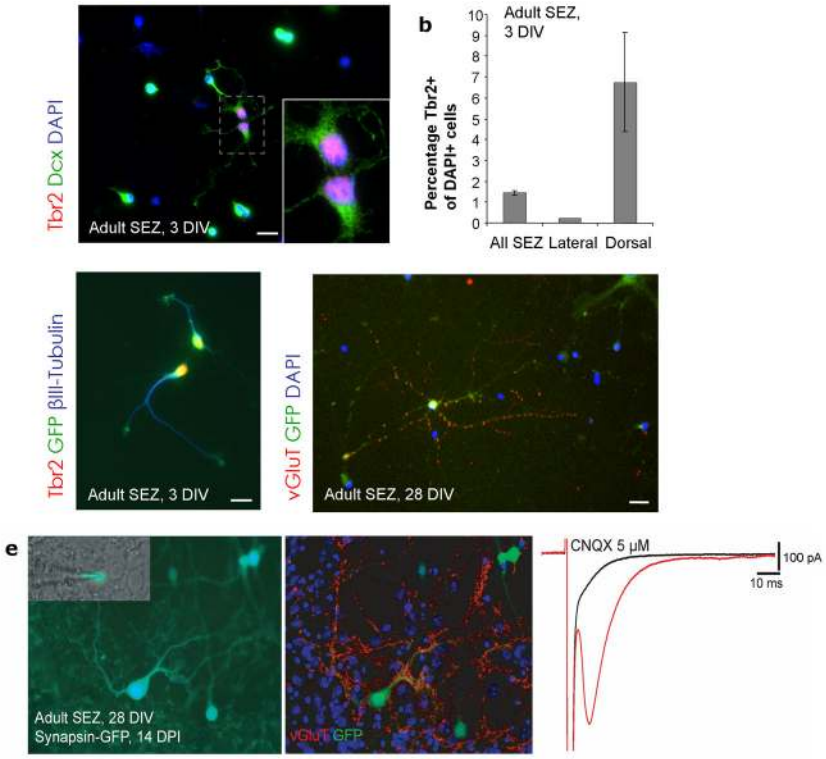

Figure 7. Adult SEZ stem and progenitor cells give rise to some glutamatergic neurons *in vitro*

(**a**) Example of two SEZ neuroblasts expressing Dcx (green) and Tbr2 (red) after 3 days *in vitro* (3 DIV). Boxed area shows Tbr2-positive nuclei at higher magnification in the lower right corner of the panel. (**b**) Quantification of Tbr2-positive nuclei in cultured SEZ stem and progenitor cells isolated from the dorsal, lateral or both walls of the lateral ventricle after 3 days *in vitro*. Tbr2-positive cells are enriched in cultures derived from the dorsal SEZ. (n = 3 experiments; dorsal cultures 471 cells, ventral cultures 602 cells, and mixed cultures 1384 cells counted, error bars are presented as s. e. m.) (**c**) Cells double-positive for Tbr2 (red) and βIII-Tubulin (blue) originate from proliferating progenitors as indicated by the transduction with a GFP-encoding retrovirus shortly after plating. (**d**) vGluT (red) immunoreactivity was also detected in GFP-positive cells 4 weeks after retroviral transduction indicating their origin from proliferating progenitors.

(**e**) Left: micrograph shows an adult SEZ derived glutamatergic neuron transduced with a lentiviral vector expressing GFP under the *synapsin* promotor that was patched by the recording electrode (inset); middle: immunostaining for vGluT and GFP after recording shows that this cell is highly decorated with vGluT positive puncta; right: stimulation of the neuron evoked an autaptic response that was blocked by the AMPA/kainate receptor antagonist CNQX revealing its glutamatergic nature.

Nuclei are visualized with DAPI (**a,d**). Scale bars: 20 μm

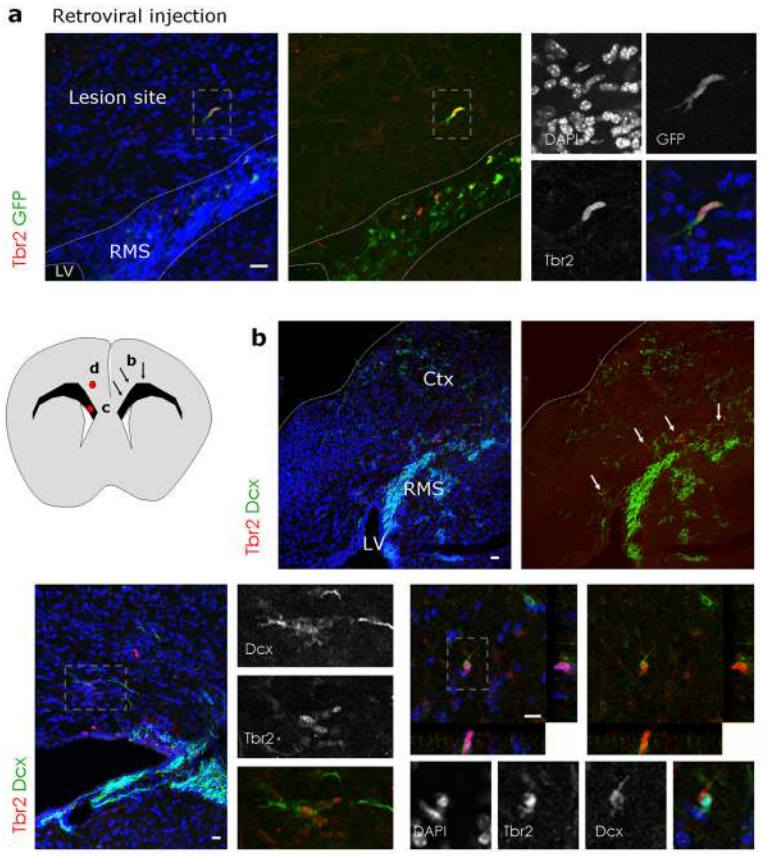

Figure 8. Tbr2-positive cells migrate into the lesioned cerebral cortex

(**a**) Retroviral injections of GFP encoding vectors 2 days prior to laser illumination result in GFP-positive cells that migrated away from the RMS 3 – 4 days after lesion, some of which are Tbr2-immunoreactive (red).

(**b**) Fluorescence micrograph depicting Tbr2- and Dcx-immunopositive cells in an overview of the lesioned cerebral cortex hemisphere and the RMS one week after Chlorine e_6 induced lesion. The schematic drawing to the left depicts the location of the arrows in **(b)** on the right side and the location of the micrographs (**c,d**) on the left side. Tbr2-and Dcx-positive cells are present in dorsal regions of the SEZ/RMS (white arrows in (**c**)) and are sometimes found in small clusters (**c**) or in the cortical grey matter (**d**). Boxed areas (grey) are shown at higher magnifications. Nuclei are visualized with DAPI (**a–d**).

Ctx = cortex, LV = lateral ventricle, RMS = rostral migratory stream, scale bars: (**a,c,d**) 20 μm, (**b**) 50 μm.